An innovative magnetorheological damper for automotive suspension: from design to experimental characterization

To cite this article: Sadok Sassi *et al* 2005 *Smart Mater. Struct.* **14** 811

INSTITUTE OF PHYSICS PUBLISHING SMART MATERIALS AND STRUCTURES

Smart Mater. Struct. **14** (2005) 811–822 doi:10.1088/0964-1726/14/4/041

An innovative magnetorheological damper for automotive suspension: from design to experimental characterization

Sadok Sassi[1], Khaled Cherif[2], Lotfi Mezghani[3], Marc Thomas[4,5] and Asma Kotrane[4]

[1] Department of Physics and Instrumentation, Institut National des Sciences Appliquées et de Technologie, Centre Urbain Nord, BP 676, 1080 Tunis Cedex, Tunisia
[2] Institut National de Recherche et d' Analyse Physico-Chimique, Pôle Technologique de Sidi Thabet, 2020 Ariana, Tunisia
[3] Société Industrielle d'Amortisseurs, Zone Industrielle Bir El Kasaa, Ben Arous, Tunisia
[4] Department of Mechanical Engineering, École de Technologie Supérieure, 1100, Notre-Dame West Street, Montreal, QC, H3C 1K3, Canada

E-mail: sadok.sassi@insat.rnu.tn, khaled.cherif@inrap.rnrt.tn, Lotfi.mezghani@sia-am.com and marc.thomas@etsmtl.ca

Received 18 February 2004, in final form 16 March 2005
Published 28 July 2005
Online at stacks.iop.org/SMS/14/811

Abstract
The development of a powerful new magnetorheological fluid (MRF), together with recent progress in the understanding of the behavior of such fluids, has convinced researchers and engineers that MRF dampers are among the most promising devices for semi-active automotive suspension vibration control, because of their large force capacity and their inherent ability to provide a simple, fast and robust interface between electronic controls and mechanical components.

In this paper, theoretical and experimental studies are performed for the design, development and testing of a completely new MRF damper model that can be used for the semi-active control of automotive suspensions. The MR damper technology presented in this paper is based on a completely new approach where, in contrast to in the conventional solutions where the coil axis is usually superposed on the damper axis and where the inner cylindrical housing is part of the magnetic circuit, the coils are wound in a direction perpendicular to the damper axis. The paper investigates approaches to optimizing the dynamic response and provides experimental verification.

Both experimental and theoretical results have shown that, if this particular model is filled with an 'MRF 336AG' MR fluid, it can provide large controllable damping forces that require only a small amount of energy. For a magnetizing system with four coils, the damping coefficient could be increased by up to three times for an excitation current of only 2 A. Such current could be reduced to less than 1 A if the magnetizing system used eight small cores. In this case, the magnetic field will be more powerful and more regularly distributed. In the presence of harmonic excitation, such a design will allow the optimum compromise between comfort and stability to be reached over different intervals of the excitation frequencies.

(Some figures in this article are in colour only in the electronic version)

[5] Author to whom any correspondence should be addressed.

1. Introduction

1.1. Magnetorheological (MR) fluid characteristics

Magnetorheological fluids (MRF) are materials that contain micron-sized, magnetically polarized particles suspended in a carrier fluid such as silicon or a mineral oil. MR fluids respond to an applied magnetic field with a change in rheological behavior. When not activated, a MR fluid behaves as ordinary oil. When it is exposed to a magnetic field, micron-size iron particles that are dispersed throughout the fluid align themselves along magnetic flux lines within milliseconds and the flow characteristics of these non-Newtonian MR fluids change by several orders of magnitude.

Recently found MR fluids have many attractive features, including high yield strength, low viscosity and stable hysteretic behavior over a broad temperature range [1–3]. However, the principal handicap of such fluids and the barrier to their widespread commercial acceptance in many areas is still their relative high cost.

Controllable fluids such as electrorheological (ER) and magnetorheological (MR) fluids have recently attracted extensive interest because of their quick response, reversible behavioral changes when subjected to electric or magnetic fields. In the past decade, diverse ER/MR damping devices have been developed for research and industrial applications [4–6]. These devices usually work according to one of three flow modes or some combination of them: the shear mode (Couette flow), the flow mode (Poiseuille flow) and the squeeze mode.

Many innovative ideas have been proposed, and new devices have been designed taking advantage of these fluids. Among those, the MRF damper represents one of the most promising devices for the structural control of civil engineering structures. To prove the scalability of MR fluid technology to devices of appropriate size for civil engineering applications, a 20 ton MR fluid damper has been designed and built [7, 8]. The damper uses a particularly simple geometry in which the outer cylindrical housing is part of the magnetic circuit. The effective fluid orifice is the entire annular space between the piston outside diameter and the inside of the damper cylinder housing.

Controllable shock absorbers can potentially be used in a variety of other mechanical systems such as automotive engines and sports equipment. Most recently, even the military has shown interest in using MR dampers to control gun recoil on naval gun turrets and field artillery. Controllable MR fluid devices have equally been tested for braking wind turbines [9] and in domestic appliances such as washing machines [10], joysticks, steering wheels and for furniture positioning, latching and locking elements as well as a host of automotive applications.

1.2. Overview of magnetorheological dampers for automotive use

When exceeding certain limits, vibrations can cause poor ride quality and stability resulting in severe damage to vehicle elements and/or passengers. Recent studies agree that chronic shock exposure increases the risk of spinal injury and lower back pain for occupational drivers and may lead to disk degeneration [11]. Conventional suspension system designs, containing passive dampers, have reached their practical limits towards achieving the optimum compromise between ride comfort and road handling and their characteristics cannot be adapted to varying road profiles. On the other hand, semi-active MRF dampers, which consist of a conventional spring and an adaptive damper, are capable of changing their response on demand and can provide the same performance as active suspensions without high power consumption and with only minor design variations from conventional passive systems.

Recently, many types of semi-active ER or MR dampers have been proposed for the vibration attenuation of various dynamic systems including vehicle suspensions [12]. Early in 1998 a commercial vibration control system based on linear MR fluid shock absorbers became available for use in the seats of large Class 8, eighteen-wheeler, trucks [13]. In 1999, MR fluid based adjustable shock absorbers for stock car and drag race vehicles were introduced [14]. In one of the most interesting works, a new way of using MR fluids in which the fluid is contained in an absorbent matrix was developed [15, 16]. Such 'MR sponge' devices contain MR fluid that is constrained by capillary action in an absorbent matrix such as a sponge or open celled foam. The sponge is used to keep the MR fluid within the active area of the device where the magnetic field is applied. The sponge allows a minimum volume of MR fluid to be operated in a direct shear mode without seals, bearings or precision mechanical tolerances. Sponges are not susceptible to gravitational settling or sedimentation of the MR fluid suspension.

In a study developed at the University of Nevada [17], a new MRF damper design for high mobility multi-purpose wheeled vehicles (HMMWV) was proposed. The semi-active MRF damper was designed to deal with a rough road environment. The fixed gap between two parallel disks was used as the magnetorheological (MR) valve. This MR valve was designed to produce higher MR forces as compared to a channel cross-section MR valve. Three-dimensional electromagnetic finite element analysis and a fluid mechanics based model were used to predict the behavior of the MRF damper.

1.3. Modeling and control of MR dampers

Alongside experimental work, the modeling of ER/MR devices has become an important aspect of research and applications. To take full advantage of the unique features of the MR damper in structural control applications, a model must be developed that can accurately reproduce the behavior of the MR damper. Significant work has been done on modeling the dynamic characteristics of MR devices, through a variety of approaches [18–21]. Numerous experimental researches have shown that unwanted system vibrations can be electively controlled through the use of ER/MR dampers associated with appropriate control strategies. One of the very important factors for achieving desirable control performance is to have an accurate damping force model which can capture the real damper behavior.

The Bingham model is the model most commonly used for describing the constitutive relations of ER/MR fluids and devices. Masri *et al* [22] proposed a curve fitting technique

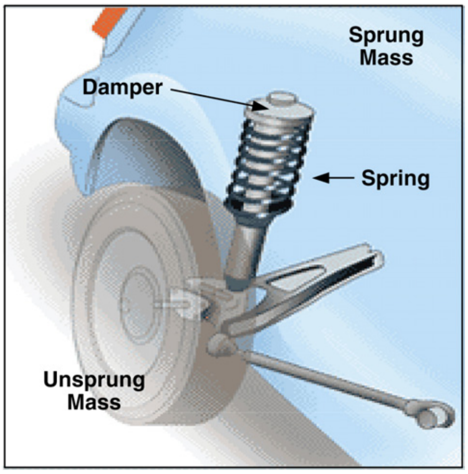

Figure 1. Vehicle suspension.

for representing the nonlinear restoring force of an ER device. Gavin *et al* [23] extended the curve fitting technique to deal with variable electric fields in modeling ER dampers. Spencer *et al* [24] developed an improved Bouc–Wen model to represent MR dampers. Wereley *et al* [25] proposed an identification procedure for ER and MR dampers by taking the equivalent viscous damping model, nonlinear Bingham plastic model, nonlinear bi-viscous model and nonlinear hysteretic bi-viscous model as underlying model structures.

Most recently, Lee and Choi presented a paper dealing with the control characteristics of a full-car suspension featuring a semi-active MR fluid damper [26]. The MR damper was applied to a full-car model. The governing equations of motion, which include vertical, pitch and roll motions, were derived and incorporated with a skyhook controller. Control characteristics of the full-car suspension installed with the proposed MR damper were evaluated through hardware-in-the-loop simulation (HILS), and presented in both time and frequency domains. It has been shown through bump and random tests that both ride quality and steering stability could be substantially improved by employing the proposed semi-active suspension system. Similar work done by Choi *et al* [27], on the vibration control of a MR seat damper for commercial vehicles, converged to the same conclusions.

2. Design details

A vehicle suspension traditionally consists of a spring and a damper mounted in parallel. The spring supports the static weight of the mass, while the damper dissipates the energy from disturbances. As displayed in figure 1, the damper and the spring are interposed on a vehicle between its sprung mass (vehicle body) and unsprung mass (wheels and wheel structures).

2.1. Conventional twin-tube hydraulic damper

The damping force created inside the damper is the result of viscous friction arising from the passage of the working fluid through an orifice. The resulting level of the damping force is a function of properties of both the orifice and the fluid. The conventional twin-tube damper contains two fluid reservoirs, one inside the other. This configuration, represented in figure 2, consists of a rod structure (1) secured to a piston (3) with transverse holes providing fluid communication between an upper ‘rebound’ chamber (V1) and a lower ‘compression’ chamber (V2). The piston moves back and forth inside a metal cylindrical inner housing (6). This inner housing is entirely filled with fluid, in such a way that no air pockets are left trapped inside. A metal cylindrical outer housing (5), partially filled with fluid, accommodates changes in volume due to piston rod movement. The outer shock tube has multiple functions, including protection of the damper’s internal parts, housing the fluid and transferring heat from the damper fluid to the surroundings. In practice, a valve assembly called a ‘foot valve’ (4) is attached to the bottom of the inner housing to regulate the fluid flow between the two reservoirs and to allow fluid communication between inner and outer housings.

2.2. Classical twin-tube magnetorheological dampers

To date, a number of experimental studies have been conducted to analyze the MR damper functionality, to improve their construction and to optimize their component design. In particular, a modeling paper written by Wereley and Pang [28] explained in detail how damping forces are developed in an annular bypass via Couette (shear mode) flow, Poiseuille (flow mode) flow or combined Couette and Poiseuille flow (mixed mode).

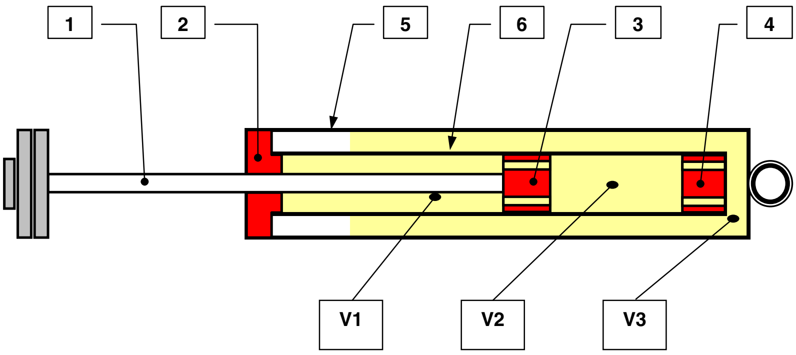

Figure 2. Conventional passive twin-tube hydraulic damper.

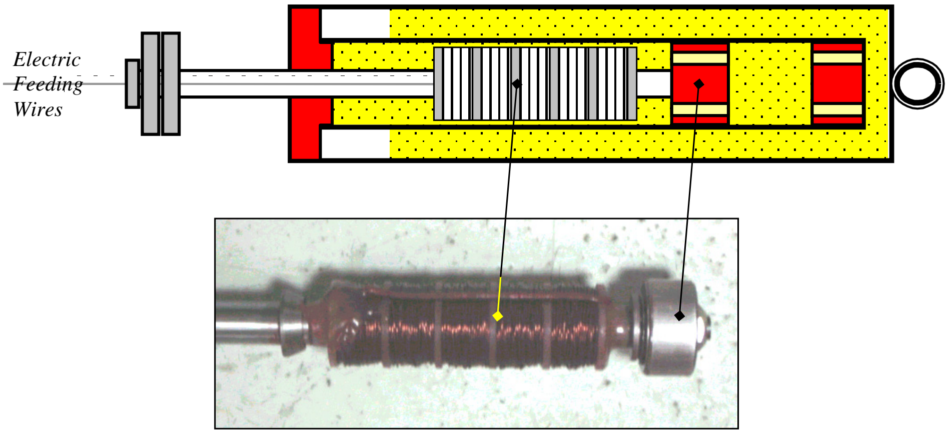

Figure 3. Classical magnetorheological bi-tube hydraulic damper.

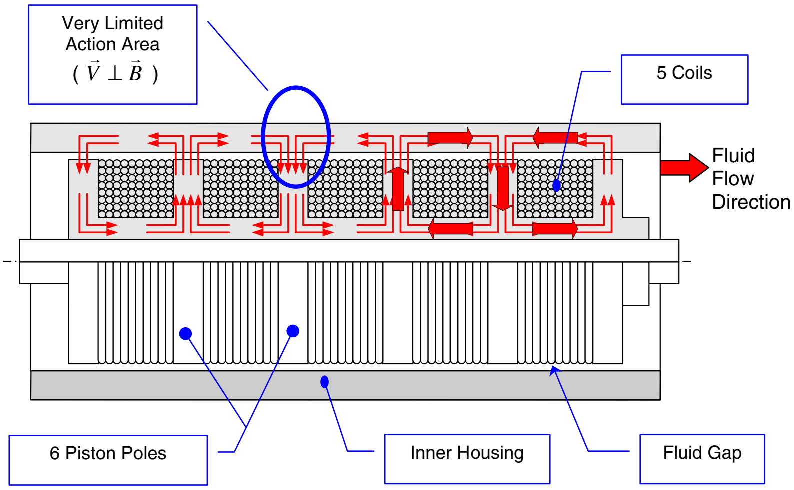

Figure 4. Flux intensity and directions in a conventional MR damper.

Figure 3 of this paper illustrates the conceptual design of the most commonly used (classical) MR twin-tube damper. Some of the parts that the conventional MR damper has in common with a passive conventional twin-tube damper are the outer and inner shock tubes, the piston ring and head, the piston rod and dynamic seals. As the piston assembly translates within the damper body tube, MR fluid is allowed to move around or through the piston assembly through a flow gap to the opposite portion of the damper body tube. A magnetic field passing across the flow gap changes the viscosity of the MR fluid in the flow gap. The flow gap thus provides shear surfaces to react to the viscosity of the MR fluid to provide damping.

The design challenge is to create a DC electromagnetic circuit that can generate sufficient flux across the MR gap in a minimum amount of time. Therefore, the difference between the rod structure in the conventional MR damper and the rod structure that is used in a conventional passive damper is that the MR rod structure has to allow for the passage of two wires which feed each of the electromagnetic coils with DC current.

As conventional drilling techniques are only able to give relatively short holes (L/D = 5–10), and in order to allow this wire passage, innovative drilling techniques should be specially developed in these cases to drill very long holes similar to the one shown in figure 3 where $L/D = 60$. This particular prototype was one of the first attempts in this long-term work, aiming to develop intelligent dampers for the semi-active control of car suspensions.

MR dampers utilize the current flowing through the damper coil to generate a magnetic field and thus a yield stress in the MR fluid. The current can be provided by either a voltage source or a current driver. The coils are housed within an intermediate isolating component. When the coils are energized, they create a magnetic field whose flux lines are shown in figure 4. To close the magnetic loop (from one pole to another) in each coil, those flux lines flow axially through the cylinder wall, radially through the six piston poles, across the fluid gap in which the MR fluid flows and then axially back through the steel core. Adjacent spools are wound in opposing directions and the magnetic flux forms five magnetic circuits. The benefit of using five different coils, instead of one single and long coil, is that the overall inductance of the circuit is much lower and consequently the time response is shorter [29]. The benefit of alternating the polarities is to strengthen the magnetic field present between two adjacent cores through the piston poles.

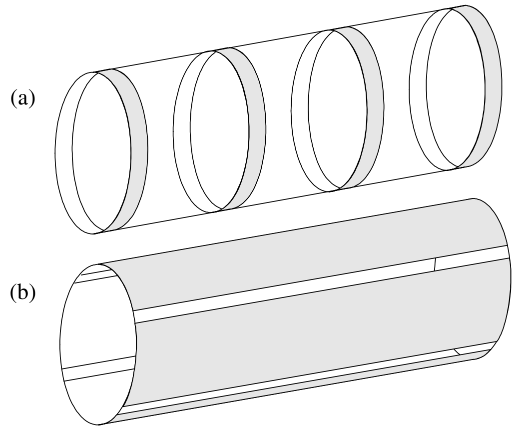

Figure 5. Active area where the fluid flow orientation is perpendicular to the magnetic flux lines: (a) old design, (b) new design.

As the increase in the resisting (damping) force is due to the chain-like formation of ferrous particles (MRF build-up) through the fluid gap and along the flux lines, one can see that the main handicap of this design is the fact that the space where the fluid flow is perpendicular to the flux lines (between two adjacent cores and toward the piston poles) is relatively small compared to the overall damper sizes (figures 4 and 5).

2.3. New design for twin-tube magnetorheological dampers

The main idea of this new design is that increasing the damping performance of any MR fluid damper depends in part upon concentrating the magnetic field at the flow gap, and/or increasing the active surface where the fluid flow is perpendicular to the magnetic flux.

An optimal design for the magnetic circuit requires maximizing magnetic field energy in the fluid gap while minimizing the energy lost in the steel flux conduit and non-working areas. Therefore, a new magnetizing system is adopted where the coils are housed within an intermediate longitudinal flux pole piece and wound perpendicularly to the symmetric axis of the damper. When the coils are energized, they create a magnetic field normal to the fluid flow direction on a relatively wide surface. Flux lines and field directions are clearly shown and explained in figures 5 and 6.

The magnetic flux path is settled radially across the gap between the pole shell and the inner housing. This particular arrangement provides a larger active area, where the required condition of perpendicular field flow orientations is assured, and significantly increases the adherence of the formed chain-like ferrous particles to the metallic surfaces. Depending on the size and length of the piston, the new design could provide a gain in the active surface to 5–10 times bigger than the one for the traditional design.

As shown in figure 7, three different magnetic circuits containing two, three and four flux pole pieces have been considered and tested. As efficient concentration of the magnetic field at the flow gap requires, in part, an efficient magnetic flux return path, we can readily conclude that poles must be used in pairs. One beneficial feature of using two double poles is that this system conducts magnetic flux better than other configurations.

In order to reduce the loss due to 'eddy currents', a sheet core has been used. Such a core is composed of 65 washers of 2 mm thickness, 34 mm external diameter and 10 mm internal diameter, shaped and welded together in order to obtain the shape shown in figure 8. The four external components of the pole shell are cut directly from a 35 mm external diameter cylindrical shell. The final magnetic pole is obtained by a combination of spot and transverse fillet welding of the 65 washers making the sheet core and the pole shells.

2.4. Electromagnetic coils

The electromagnetic force is proportional to the product of the number of turns around the core in which the flux is to be established, and the current circulating through the turns of wire. This clearly indicates that an increase in the number of turns or in the current through the wire will result in an increased 'pressure' on the system to establish flux lines through the core. However, an increase in the number of turns requires a smaller wire section which, in turn, allows less current, and vice versa.

A compromise between these two parameters should be found. After several trials, it was established that the most appropriate wire section was 0.355 mm. The available internal space inside the new MR damper allows 120 turns per pole for the two-magnetic-pole system, 100 turns per pole for the three-magnetic-pole system or 80 turns per pole for the four-magnetic-pole system. For the last case, a current of 1 A

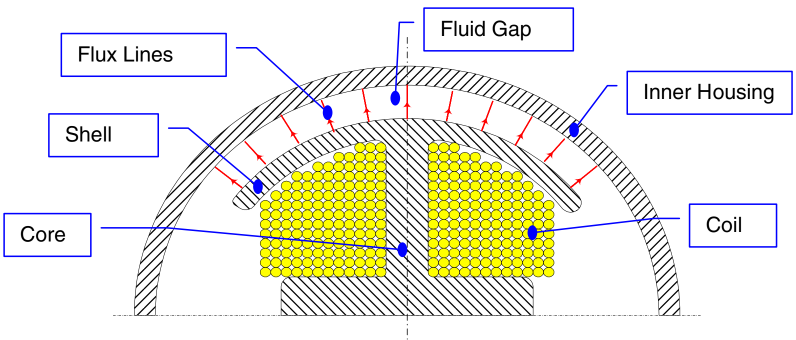

Figure 6. Flux intensity and directions in the new MR damper.

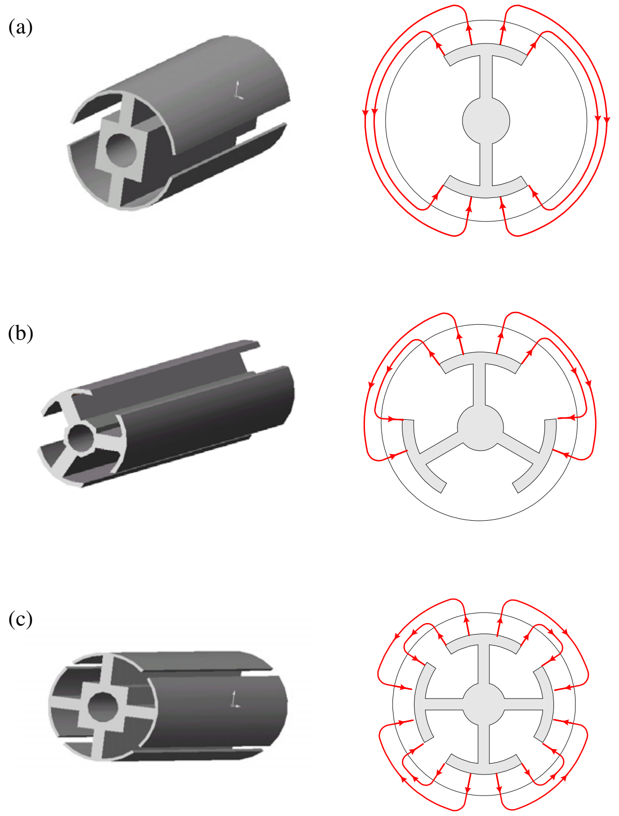

Figure 7. Flux intensity and directions for different magnetic pole configurations. (a) Two magnetic poles, (b) three magnetic poles, (c) four magnetic poles.

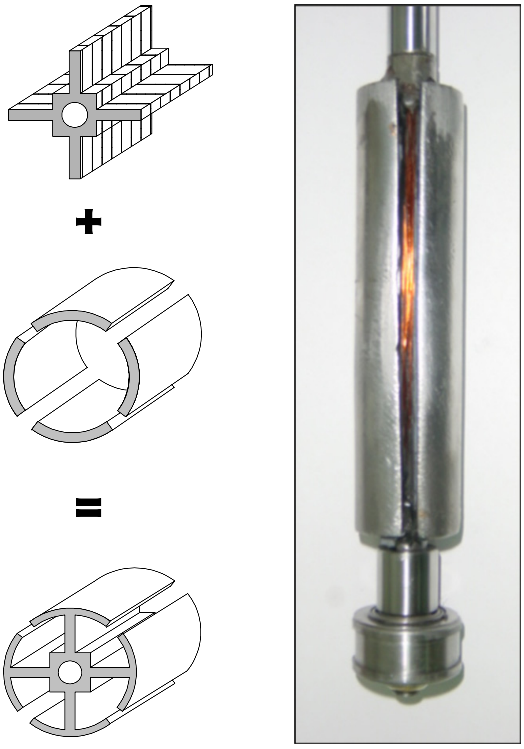

Figure 8. Shape of the magnetic sheet core and external shell.

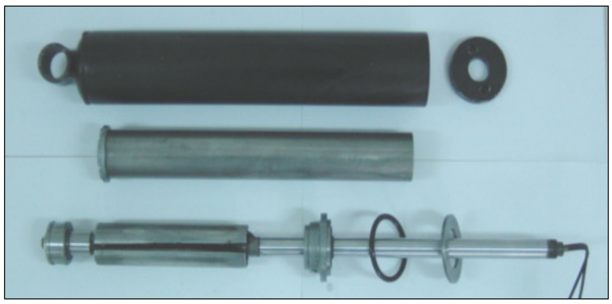

Figure 9. Different components of the new MR damper.

traversing the coils may induce a power loss due to heat dissipation around 18 W. As the excitation is not permanent, this induced warming remains tolerable and without leading severe effects or damage for the sealing and the rest of the internal components. As a matter of fact, for standard applications, the current density of copper wires may vary from 4 to 8 A mm^{-2}, depending on the type of isolation, the type of environment and the type of cooling device (this is equivalent to a current of 0.35–0.7 A for a wire of 0.335 mm diameter). However, for special applications corresponding to intermittent excitation in a 'friendly' environment, as in our case where the presence of fluid all around the coils contributes to evacuation of the heat generated, the coils can tolerate a current density up to 20 A mm^{-2} (equivalent to a current of 1.8 A for a wire of 0.335 mm diameter) for a short duration.

The next step was to decide on the kinds of dampers to use for the new magnetizing device to build up the new MR damper. After carefully analyzing the different kinds of dampers available, their internal mechanisms, their components and their possible adaptabilities, it was decided that the most suitable model, offering enough internal space to bring about modifications without serious technical problems, is the one corresponding to a truck. The entire MR damper development effort was focused on minimal cost, minimal transformations and simplicity of design. The prototype developed in this study, and represented in figure 9, has a piston with an overall length of 18 mm and an external diameter of 35.7 mm.

The metal cylindrical outer housing used on conventional truck dampers is usually of type 60/1.5, which corresponds to an external diameter of 60 mm and a thickness of 1.5 mm. As the replenishment and the draining of oil are very frequent operations during the tests, it was of interest to have a removable cover. To allow manufacture of a threaded end, it was necessary to increase the thickness of the body to at least 2.5 mm. The damper external body was then chosen to be of type 60/2.5. Moreover, to cut the experiment costs, the length of the body was shortened to 320 mm to limit the amount of expensive MR fluid inside the damper.

The damper contains approximately 420 ml of MR fluid. The amount of fluid energized by the magnetic field at any given moment is approximately 8 cm^3.

Among several problems met during the manufacturing and the assembling of the MR damper, the most important one was fluid leakage. Several types of glue were tested before the final selection of the right one.

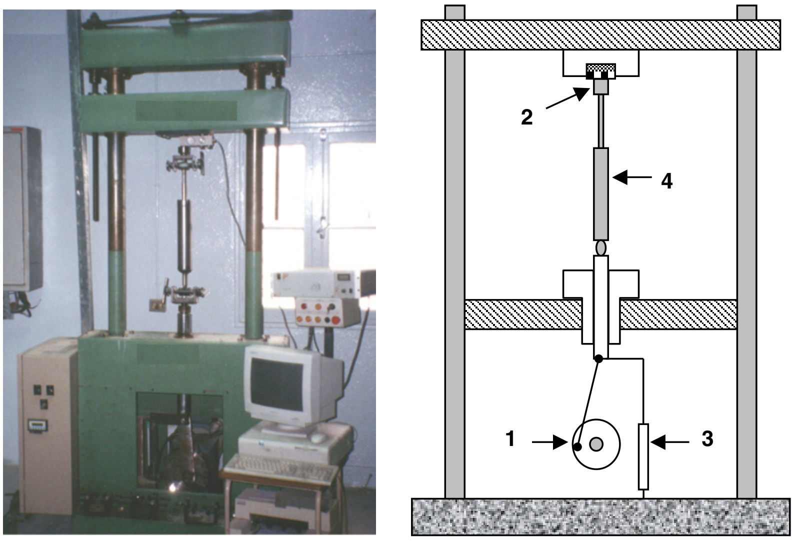

Figure 10. Shaking table testing and experimental set-up.

3. Laboratory facility and experimental set-up

A mechanically activated shaking table was specially designed to provide a laboratory facility for performing vibration control experiments. The load frame shown in figure 10 was designed and built for the purpose of obtaining the MR damper response data necessary for identification studies.

In this set-up, an eccentric actuator (1), coupled to a crank rod system, was employed in order to drive the shaking table holding the damper. A linear variable differential transformer (LVDT) (3) was used to measure the displacement of the piston rod of the ER damper (4), and a load cell (2) with a range of 1000 daN was included in series with the damper to measure the output force. The data acquisition system employed consisted mainly of a computer and the '*LABTECH Realtime VISIONpro*' software. Using this experimental set-up, the response of the damper can be measured for a wide range of prescribed speeds.

4. Experimental results

Using the set-up depicted in figure 10, preliminary tests were conducted to measure the response of the damper under various loading conditions. In each test, the new MR damper was driven with harmonic signals at different fixed frequencies, and a constant level of current applied to the coils of the MR damper.

The damper should function properly as long as the valving is set up properly. The design of the valving system and the choice of its mechanical components are perhaps among the most important and delicate steps. The failure of the whole system could be caused simply by the use of a wrong washer thickness or spring rigidity. An ideal valving system must be rigid enough to stop the fluid communication between the chambers in one way, and at the same time soft enough to allow the fluid motion in the opposite direction when the rod is driven into motion.

Filling the damper with the MR fluid is also a delicate operation because of the importance of proportions of air (at the top of the outer cylinder) and fluid (inside the whole inner cylinder and some of the outer cylinder). Filling the damper with the wrong air/fluid proportions may induce an inadequate functioning characteristic. Moreover, if a filling operation is not carried out correctly, some air 'pockets' may remain trapped inside the fluid. In the twin-tube damper configuration, it is necessary for the air to remain at the top of the outer cylinder. If the air does not remain at the top of the damper and passes through the damper valving, the damping effect is significantly diminished, as in the case where the fluid cavitates. This phenomenon is easy to detect as it is characterized by a highly distorted force–displacement loop.

The MR damper was filled with 'MRF 336AG', developed by LORD [30]. Using this professional fluid, a wide range of piston linear speeds and current levels were considered and tested. When the DC generator is turned OFF, and for a specific displacement amplitude $a = 250$ mm, the force versus displacement for different speeds V, ranging from 0.065 to 0.419 m s^{-1}, is shown in figure 11. As can be seen in figure 12, the damping force F (N) is found to be a combination of friction and viscous damping and can be expressed as

$$F\ (\text{rebound}) = 8168\ V + 14 \tag{1}$$

$$F\ (\text{compression}) = 2150\ V - 835. \tag{2}$$

The upper part of the curve, corresponding to positive speeds, is related to expansion, while the lower part, corresponding to negative speeds, is related to compression. Using this plot, the damping coefficient C was obtained from the slope of the best linear curve fitting the experimental points: $C_{\text{rebound}} = 8169$ N s m^{-1} and $C_{\text{compression}} = 2150$ N s m^{-1}.

When the generator is turned ON, the effect of the applied current is readily observed. As represented in figure 13, it can be observed that the rebound damping coefficient follows a third-order polynomial curve with the applied current feeding the electromagnet coils (coefficient of determination: 94%).

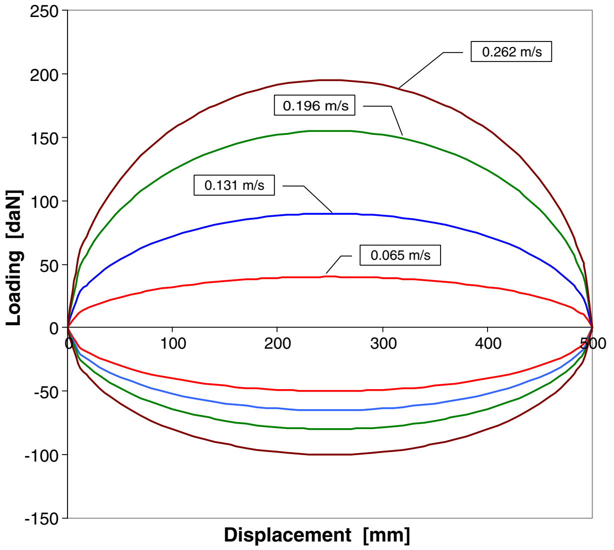

Figure 11. One cycle of force versus displacement, for different speeds, when the DC power is OFF.

5. Simulation and numerical results

The profiles of the roads on which the vehicles are taken for movement tests present numerous irregularities, with the size, shape and frequency of appearance varying according to the type of network considered and the quality of the coating. Working on a prototype, it was very important, firstly, to verify its performances and, secondly, to optimize them. The dynamics of this new model of MR dampers were analyzed by computer, with an emphasis on the evaluation of the influence of electrical current on the resulting dynamic response. Because a rolling vehicle can encounter four kinds of soil excitations, i.e., *Step* (abrupt rise of soil), *Impulse* (abrupt rise with immediate abrupt falling down), *Harmonic* (periodic obstacles of repeated sinusoidal shape) and *Random*, the characteristics of a car suspension equipped with the MR damper should be numerically tested for such types of road excitation.

5.1. Mathematical model

To examine vibration isolation and road holding characteristics, an analysis can be performed using a simplified car model (figure 14). The car suspension may be considered as a system with one degree of freedom, a much simplified model that retains many of the essential characteristics of more complex systems in its response to excitation. In this simple idealized model, a mass M is supported by four springs K in parallel with four viscous dampers C.

Ride comfort can be evaluated by the response of the sprung mass to excitation from the ground. Road holding is related to the variation of the force between the road and the wheel during vibration.

The movement equation of such a system is written in the following form:

$$M\ddot{x}(t) + 4C_i[\dot{x}(t) - \dot{y}(t)] + 4K[x(t) - y(t)] = 0$$
$$\text{where: } C_i = C_{\text{rebound}} \quad \text{when } V > 0$$
$$C_i = C_{\text{compression}} \quad \text{when } V < 0. \tag{3}$$

$x(t)$ is the displacement of the car body, $y(t)$ is the displacement of the wheels. M is the mass of the truck (20 000 kg $\approx$ 44 000 lb), K is the stiffness of the spring that could be used with our prototype, with a value of about 150 000 N m^{-1}, and C is the value of viscous damping which is derived from the experimental results as shown above in figure 12.

5.2. Simulation results

5.2.1. Response due to a shock excitation. When the car suspension encounters an abrupt rise with an immediate abrupt falling down, the car body will be excited by an *impulsive* force.

The system, being disturbed from its equilibrium position, will start oscillating. The oscillation amplitude will decrease progressively until the system regains its initial position.

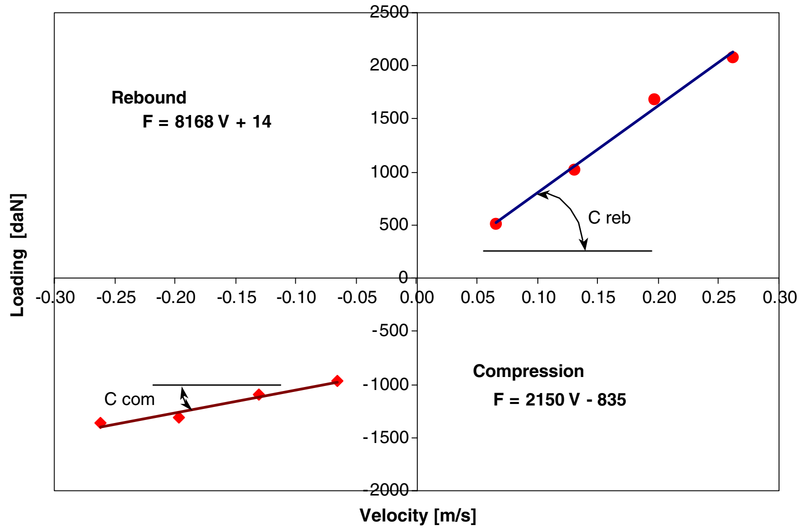

Figure 12. Force versus velocity, when the DC power is OFF.

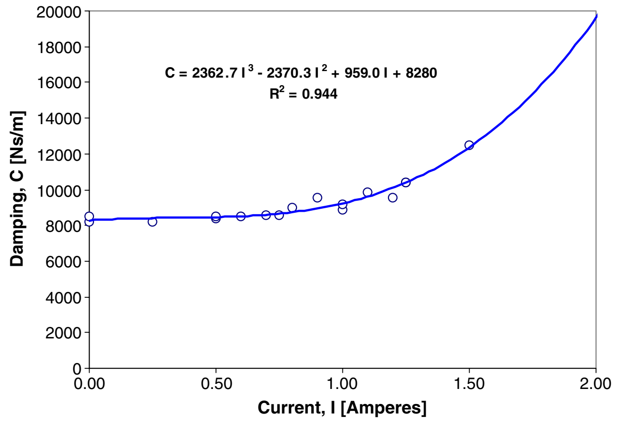

Figure 13. Measured rebound damping coefficient versus applied electric current.

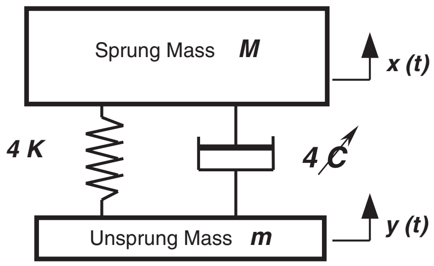

Figure 14. One-DOF car model.

Figure 15 shows the rate of decay of such damper-free oscillations, as simulated by MATLAB. The results with and without coil electrical excitation are printed on the same graph. Without electrical excitation the damping rate ζ, defined as $\zeta = \delta/\sqrt{4\pi^2 + \delta^2}$, where δ is the logarithmic decrement, is initially around 10%. By exciting the coil with a current of 1.25 A, the logarithmic decrement could be increased from $\delta(0\ \text{A}) = 0.522$ to $\delta(1.25\ \text{A}) = 0.630$, which corresponds to a damping rate of 11.55%. Such improvement is certainly not enough to make a noticeable difference between the ON and OFF states of the excitation. However, when the current is set to a value equal to 2 A, the simulation results represented in figure 15 show that the logarithmic decrement could be increased to $\delta(2\ \text{A}) = 1.132$, which corresponds to a damping rate of 20.7%.

Figure 16 describes the effect of the excitation current on the damping rate. To damp vibration efficiently, a damping rate of 70% is normally sufficient and can be considered as optimal, because any higher damping value would be useless. Figure 16 shows that this damping rate corresponds to a current excitation of 2.9 A.

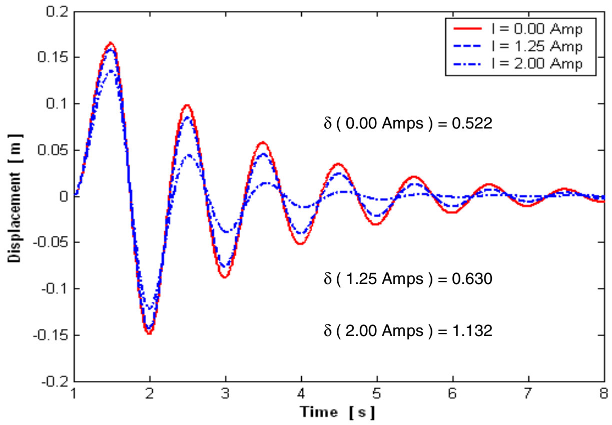

Figure 15. Numerical simulation of MR damper-free response for excitation currents of 0.0, 1.25 and 2.00 A.

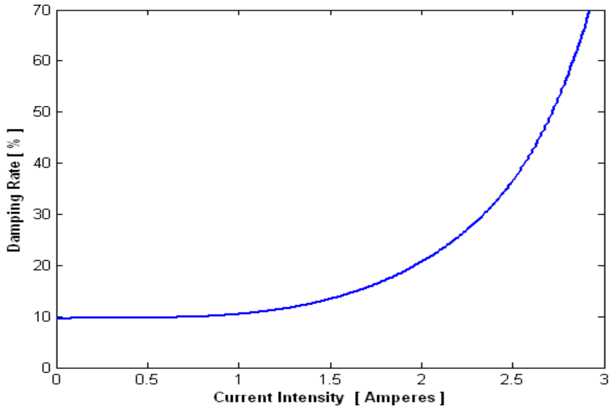

Figure 16. Improvement of damping rate with excitation current.

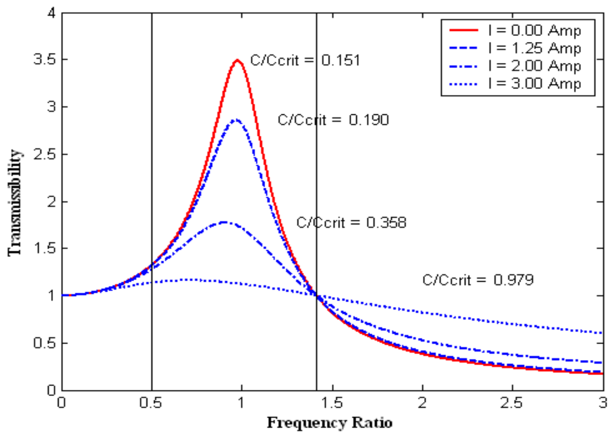

Figure 17. Transmissibility versus frequency ratios for different current values.

5.2.2. Response due to a periodic excitation. When a vehicle fitted with a MR damper is driven over an undulating road, whose contour can be approximated fairly accurately by a sine wave having a wavelength L, at a velocity V, the contour of the road acts as a support harmonic excitation on the system with an exciting frequency $\omega = 2\pi V/L$. The system response will be characterized by the transmissibility TR, defined as the ratio of the transmitted force to the excitation force, and the amplification ratio AR, defined as the ratio of the resulting motion to the excitation motion amplitude.

Figure 17 shows the displacement of the car body with respect to the input. Notice that at low damping, resonant transmissibility is relatively large, while transmissibility at

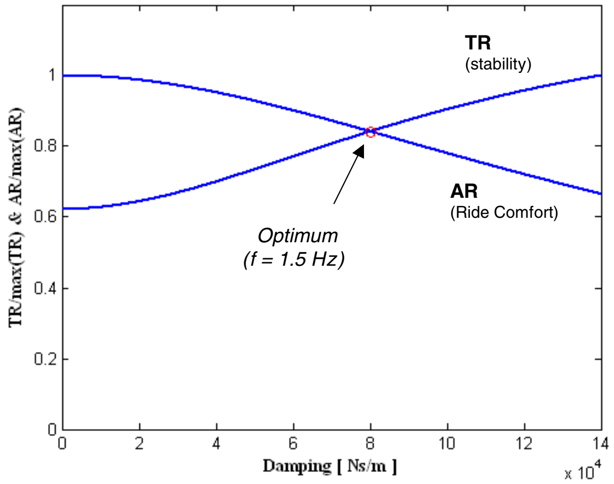

Figure 18. Dimensionless transmissibility and amplification ratio versus damping coefficient, evaluated at a frequency excitation of 1.5 Hz.

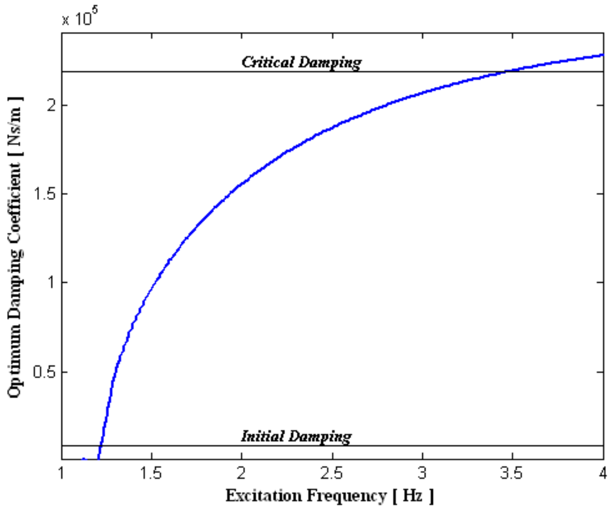

Figure 19. Optimum damping coefficient versus excitation frequency.

higher frequencies is quite low. As the damping is increased, the resonant peaks are attenuated, but isolation is lost at high frequency. The lack of isolation at higher frequencies will result in a harsher vehicle ride. This illustrates the inherent tradeoff between resonance control and high frequency isolation associated with the design of passive vehicle suspension systems.

The ways in which the transmissibility TR and amplification ratio AR are influenced by the value of the damping constant C are represented in figure 18. This figure is plotted for a 1.5 Hz excitation of the road, while the truck's natural frequency is 0.872 Hz ($\omega/\omega_n = 1.72$).

It can be noted that the damping constant of the damper determines both the stability of the vehicle and the comfort of travelers. A high damper (a damper with high damping characteristics) reduces the amplification and provides good stability, keeping the tires in contact with the road and preventing frame oscillations and other problems, but it increases the force transmissibility and will transfer much of the road excitation to the passenger, causing an uncomfortable ride. On the other hand, a soft damper (a damper with low damping characteristics) will increase ride comfort, but will equally reduce the stability of the vehicle. The design of a suspension is a compromise between stability and comfort, and an optimum level must be found.

As the optimum compromise between comfort and stability depends on the excitation frequency, as indicated in figure 19, it appears that it is impossible for a MR damper to be optimized over the entire range of frequencies. Therefore, in response to measurements made by accelerometers, the damper controller should not only impose an ON/OFF policy to produce an ON/OFF MR damping, but also be able to somehow vary the value of the MR damping effect.

6. Magnetic field

When the DC power is ON, DC current traverses the coils, generating an electromagnetic field. The flux lines traverse the shell core in the radial direction. The number of flux lines

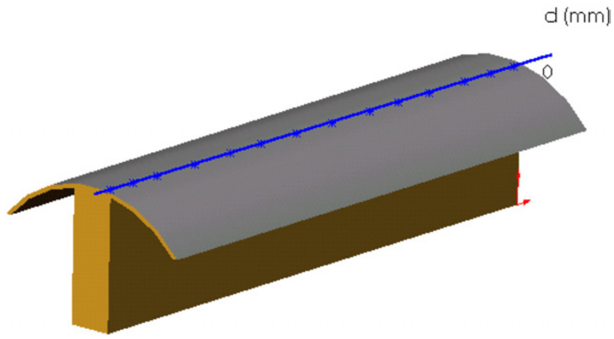

Figure 20. Measuring of flux density along the core surface.

per unit area, called the flux density and denoted by B, was experimentally measured along the tangent to the shell core external surface (figure 20).

The absolute values of the results obtained are plotted in figure 21. Surprisingly, it was found that the magnetic field profile presents a maximum at the two extremities and a wide minimum in the middle. Therefore, and contrary to what was initially expected, splitting this magnetic core into two smaller elements induced a more powerful effect. The flux density B is related to the number of flux lines Φ passing through the area A by the following equation:

$$B\ [\text{teslas}] = \frac{\Phi\ [\text{webers}]}{A\ [\text{square meters}]}. \tag{4}$$

For the same available internal space, the number of flux lines Φ could be held constant by keeping the same number of wire turns and the same current intensity. Therefore, any reduction in the traversed area induces an increase in the flux density. The numerical fitting of the experimental results and the integration of the curves related to one single core or two half-cores show that the MR expected action is doubled if the surface core is split into two elements. The new design would have a stronger value and a more regular profile.

Moreover, splitting the cores into two smaller ones, for the four-magnetic-pole system, resulted globally in eight

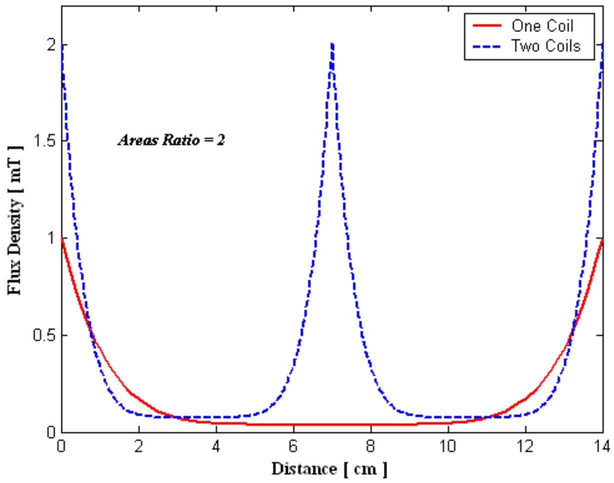

Figure 21. Flux density along the surface of one single core and two half-cores.

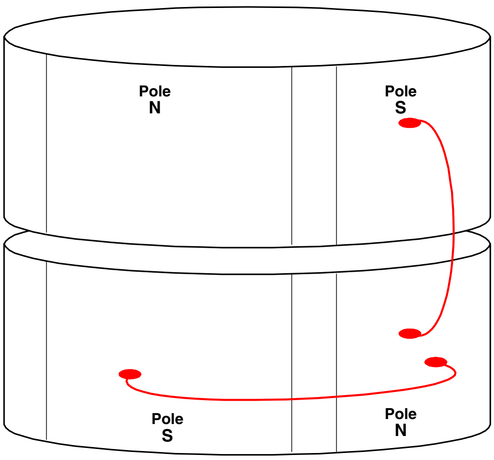

Figure 22. Flux line circulation between upper and lower coils.

independent coils. As shown in figure 22, depending on the position of the coils (upper or lower) and their types (North or South), different combinations of excitation could be obtained leading to different values of the damping coefficient, with flux lines circulating in the longitudinal direction, in the radial direction or in both directions. As each one of the coils could be excited separately, an intelligent choice of combinations of them may result in a stepped increase of the overall damping coefficient. Therefore, instead of continuously varying the current to all the eight coils to meet the condition required by figure 19, the same goal could be achieved in a stepped way by applying one single current to different combinations of coils. The overall MR modified value of the damping coefficient should at no time exceed the critical value.

7. Conclusions

This paper reports the design and the manufacture of a new MR damper based on a completely new approach where the electromagnetic axis is perpendicular to the damper axis. The paper also provides a description of the magnetizing device technology, characterization test results and optimization criteria. This new MR damper prototype was designed and fabricated on the basis of minimum component change from the original passive damper with a very close collaboration with the 'Société Industrielle d'Amortisseurs', to use for semi-active vibration control of a truck suspension.

The results obtained from laboratory tests and numerical simulations clearly show that the damping coefficient could be increased to up to three times when the exciting current inside the coils is around 2 A.

Numerical simulations show that, in the case of a harmonic excitation, the optimum compromise between comfort and stability depends on the excitation frequency. Adopting a magnetizing system with eight independent coils may require a current of lower intensity and may allow the damper to reach its optimum capacity over a wide range of frequencies.

Acknowledgments

The authors gratefully acknowledge the financial support, the technical assistance and the helpful comments and advice offered by the technical staff of the 'Société Industrielle d'Amortisseurs'. The authors gratefully acknowledge the CRSNG for financial support.

References

[1] Carlson J D, Catanzarite D M and St Clair K A 1996 Commercial magneto-rheological fluid devices *Proc. 5th Int. Conf. on ER Fluids MR Fluids and Associated Technology (University of Sheffield, UK)* pp 20–8

[2] Carlson J D and Weiss K D 1994 A growing attraction to magnetic fluids *Mach. Des.* 61–6

[3] Carlson J D 1994 The promise of controllable fluids *Proc. Actuator 94* ed H Borgmann and K Lenz (Bremen: AXON Technologies Consult GmbH) pp 266–70

[4] Stanway R, Sproston J L and El-Wahed A K 1996 Applications of electro-rheological fluids in vibration control: a survey *Smart Mater. Struct.* **5** 464–82

[5] Spencer B F Jr and Sain M K 1997 Controlling buildings: a new frontier in feedback *IEEE Control Syst. Mag.* **17** 19–35

[6] Symans M D and Constantinou M C 1999 Semiactive control systems for seismic protection of structures: a state-of-the-art review *Eng. Struct.* **21** 469–87

[7] Carlson J D and Spencer B F Jr 1996 Magneto-rheological fluid dampers for semiactive seismic control *Proc. 3rd Int. Conf. on Motion and Vibration Control (Chiba, Japan)* vol III, pp 35–40

[8] Spencer B F Jr, Yang G, Carlson J D and Sain M K 1999 Smart dampers for seismic protection of structures: a full-scale study *Proc. 2nd World Conf. on Structural. Control* vol 1, pp 417–26

[9] Oualla J, Thomas M and Lafleur F 2003 The possibilities and limitations of an MR brake in the process of braking small wind turbines *6th Int. Workshop on Smart Materials and Structures (Cansmart, Montreal)* ed G Akhras (Ontario: University of Ottawa) pp 303–14

[10] Chrzan M J and Carlson J D 2001 MR fluid sponge devices and their use in vibration control of washing machines *Proc. SPIE, Smart Structures and Materials* **4331** 370–8

[11] Thomas M, Lakis A A and Sassi S 2004 Adverse health effects of long-term whole-body random vibration exposure *Recent Research Development in Sound and Vibration* vol 2, Transworld Research Network, pp 55–73

[12] Sassi S, Cherif K and Thomas M 2003 On the development of a smart damper based on electro-rheological technology *Smart Mater. Struct.* **12** 873–80

[13] Leroy D F, Marjoram R and St Clair K 1999 Giving truck drivers a smooth ride *Mach. Des.* **71/20** S7–11

[14] Anon 1999 Magnetic fluid shocks *Mech. Eng. Mag., ASME* 32–3

[15] Carlson J D 1998 Low-cost MR fluid sponge devices *Proc. 6th Int. Conf. on New Actuators* ed H Borgmann (Bremen: Messe Bremen GmbH) pp 417–21

[16] Carlson J D 1998 New cost effective braking damping and vibration control devices made with magnetorheological fluids *Mater. Technol.* **13** 96–9

[17] Dogruer U, Gordaninejad F and Evrensel C A 2004 A new magneto-rheological fluid damper for high-mobility multi-purpose wheeled vehicle (HMMWV) *Proc. SPIE, Smart Structures and Materials 2004: Damping and Isolation* vol 5386, ed K-W Wang (Bellingham, WA: SPIE Optical Engineering Press) pp 195–203

[18] Lee D Y and Wereley N M 1999 Quasi-steady Herschel–Bulkley analysis of electro- and magneto-rheological flow mode dampers *J. Intell. Mater. Syst. Struct.* **10** 761–9

[19] Kordonsky W I 1993 Magnetorheological effect as a base of new devices and technologies *J. Magn. Magn. Mater.* **122** 395–8

[20] Spencer B F, Dyke S J, Sain M K and Carlson J D 1997 Phenomenological model for magnetorheological dampers *J. Eng. Mech., ASCE* **123** 230–8

[21] Wereley N M, Kamath G M and Madhavan V 1999 Hysteresis modeling of semi-active magnetorheological helicopter dampers *J. Intell. Mater. Syst. Struct.* **10** 624–33

[22] Masri S F, Kumar R and Ehrgott R C 1995 Modeling and control of an electrorheological devices for structural control applications *Smart Mater. Struct.* **4** A121–31

[23] Gavin H P, Hanson R D and Filisko F E 1996 Electrorheological damper, part II: testing and modeling *J. Appl. Mech., ASME* **63** 676–82

[24] Spencer B F Jr, Sain M K and Carlson J D 1997 Phenomenological model for magnetorheological dampers *J. Eng. Mech., ASCE* **123** 230–8

[25] Wereley N M, Pang L and Kamath G M 1998 Idealized hysteresis modeling of electrorheological and magneto-rheological dampers *J. Intell. Mater. Syst. Struct.* **9** 642–9

[26] Lee H S and Choi S B 2000 Control and response characteristics of a magneto-rheological fluid damper for passenger vehicles *J. Intell. Mater. Syst. Struct.* **11** 80–7

[27] Choi S B, Nam M H and Lee B K 2000 Vibration control of a MR seat damper for commercial vehicles *J. Intell. Mater. Syst. Struct.* **11** 936–44

[28] Wereley N M and Pang L 1998 Nondimensional analysis of semi-active electrorheological and magnetorheological dampers using approximate parallel plate models *J. Smart Mater. Struct.* **7** 732–43

[29] Kelso S P 2001 Experimental characterization of commercially practical magnetorheological fluid damper technology *Proc. SPIE Conf. on Smart Structures and Materials (Newport Beach, CA)* (Bellingham, WA: SPIE Optical Engineering Press) pp 292–9, Paper No. 4332-34

[30] Lord Rheonetic 2004 Magnetically responsive technology *MR Fluid Product Bulletin* (www.lord.com/mr)